ISBN: 978-3-95450-214-1 ISSN: 2673-5490 doi:10.18429/JACoW-IPAC2021-TUPAB275

ENHANCED ORTHOGONAL POLARIZATION COMPONENT TREATMENT IN COTRI MODEL FOR MICROBUNCHED BEAM DIAGNOSTICS*

D. W. Rule‡, Silver Spring, MD 20904 USA
A. H. Lumpkin†, Argonne Associate, Argonne National Laboratory, Lemont, IL 60545 USA

Abstract

We present the results of modifying our coherent optical transition radiation interferometry (COTRI) model's treatment of the perpendicular polarization of OTR, Iperp. Our previous analytic approximation for Iperp was for beam divergences, σ_y'<< 1/γ where γ is the Lorentz factor and σ_y' is the rms y-component of the beam divergence. We have replaced our analytical form with a Gaussian quadrature for the convolution of Iperp with the divergence in theta-y. This extends the range of divergences we reliably model to σ_y' > 1/ γ. Ipar, the parallel polarization in the model, is unchanged. Iperp is polarized along the y-axis and is proportional to the square of the y-component of the beam's velocity distribution. We illustrate our results with two cases: 1) beam energy E=1 GeV, OTR wavelength 633 nm, Q=235 pC, microbunching fraction, bf=1%, rms divergences σ_y' of 0.1-0.7 mrad, and rms beam sizes 2, 10, and 30 µm; 2) E=375 MeV, wavelength 266 nm, Q=300 pC, bf=10%, rms divergences of 0.1-0,7 mrad, and rms beam sizes of 10, 25, 50, and 100 µm. We will present two cases which would be of interest for the diagnostics of laser plasma accelerator beams and pre-bunched FELs, respectively.

INTRODUCTION

The model for COTR interferometry (COTRI) was first developed for the SASE-FEL-induced microbunching case [1, 2]. In one classic case, microbunching fractions reached 20% at saturation of a self-amplified spontaneous emission (SASE) FEL resulting in gains of 106 at 530 nm [2]. In that experiment the concomitant z-dependent gain of coherent optical transition radiation (COTR) was also measured at the >105 level. Microbunching at visible wavelengths in laser-driven plasma accelerators (LPAs) had been reported previously [3, 4], but it has only recently been measured in near-field and far-field OTR images on a single shot [5, 6] with significant COTR enhancements > 105. Extensive far field COTRI fringes out to 30 mrad in angle space were produced by the micron sized LPA beams.

For application to LPAs, the diagnostic model was improved by adding the capability of incorporating into the coherence function two different beam transverse profiles at the two interferometer foils in order to evaluate COTRI from the micron sized LPA beams [6]. These very small sizes necessitated that we include the relatively significant change in size due to divergence as the beam transits the interferometer. In the present paper we show how we enhanced the treatment of the perpendicular polarization $I_\perp$ by replacing an approximate expression for $I_\perp$, valid for beam divergences much less than 1/γ, by an exact numerical evaluation of the convolution of the beam divergence distribution functions into the OTR expressions for $I_\perp$.

COTRI MODEL

The COTRI diagnostic technique employs the Wartski interferometer to generate OTR interference patterns which are sensitive to beam divergence and energy, as well as to the radial and longitudinal beam distributions, in particular for the microbunched beams producing the coherent OTR of interest here.

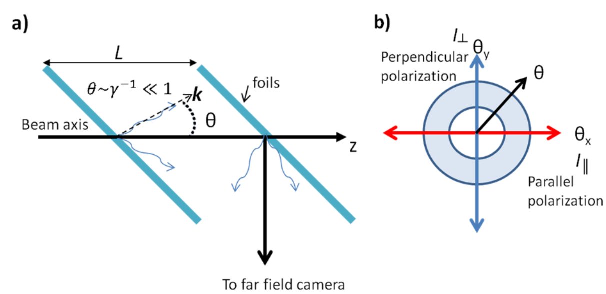

Figure 1: a) Wartski interferometer [7, 8]. b) schematic of the far field OTR interference pattern defining the $I_\parallel$ and $I_\perp$ polarizations for a scan of the image along θ_x, noting that $\theta^2 = \theta_x^2 + \theta_y^2$.

Figure 1a) shows the two foil Wartski OTR interferometer having foils at 45º to the beam axis and with spacing L. The forward directed OTR from the first foil is reflected off the back of the second foil and interferes in the far field as depicted in Fig. 1b) which defines the parallel and perpendicular polarizations for a scan along the θ_x axis.

To proceed we specialize the COTRI model to the discussion of the treatment for perpendicular polarization. The number $W_{1\perp}$of perpendicularly polarized OTR photons that a single electron generates per unit frequency ω per unit solid angle Ω from a single foil is

$$\frac{d^2W_{1\perp}(\theta_x,\theta_y)}{d\omega d\Omega} = \frac{e^2}{\hbar c}\frac{1}{\pi^2\omega}\,\beta_\perp^2\,|r_\perp|^2\,\frac{1}{(\gamma^{-2}+\theta_x^2+\theta_y^2)^2}\,, \quad (1)$$

where $|r_\perp|^2$is the reflection coefficient for perpendicularly polarized OTR reflected from the *second* foil.

*Work supported in part by U.S. Department of Energy, Office of Science, under Contract No. DEAC02-06CH11357
‡ruledw@verizon.net
†lumpkin@fnal.gov

ISBN: 978-3-95450-214-1 ISSN: 2673-5490 doi:10.18429/JACoW-IPAC2021-TUPAB275

The COTRI model, incorporating Eq. (1) for perpendicular polarization becomes,

$$\frac{d^2W_\perp}{d\omega d\Omega} = \frac{d^2W_{1\perp}}{d\omega d\Omega}\left[N\boldsymbol{I(k)} + N_b\left(N_b - 1\right)\boldsymbol{J(k)}\right], \quad (2)$$

where N_B of the total number N are microbunched, i.e. the bunching fraction, bf = N_B/N. ***I(k)*** is the expression for the interference of the OTR from the first and second foils of the interferometer, given by

$$\boldsymbol{I(k)} = 4\sin^2\left[\frac{kL}{4}\left(\gamma^{-2} + \theta_x^2 + \theta_y^2\right)\right], \quad (3)$$

where $k = |\boldsymbol{k}| = 2\pi/\lambda$. Peaks of ***I(k)*** occur at angles $\theta_x{}^2 + \theta_x{}^2 = \frac{2\lambda}{L}(p - p_0)$, where $p = 1/2,\ 3/2\ldots$ and $p_0 = L/(2\lambda\gamma^2)$. For good sensitivity to divergence p_0 should be of the order of unity. The coherence function ***J(k)*** in Eq. (2) can be defined as

$$\boldsymbol{J(k)} = \left(H_1(\boldsymbol{k}) - H_2(\boldsymbol{k})\right)^2 + H_1(\boldsymbol{k})H_2(\boldsymbol{k})\boldsymbol{I(k)},$$

where $H_j(\boldsymbol{k}) = \rho_j(\boldsymbol{k})/Q = g_j(k_x)\, g_j(k_y)\, F_z(k_z)$, for a microbunch of charge distribution $\rho_j(\boldsymbol{x})$ and total charge Q, with j = 1, 2. Here we have introduced two microbunch form factors, H_1 and H_2, to account for the increase in bunch radius from the first to the second interferometer foil due to beam divergence. Each $H_j(\boldsymbol{k})$ is a product of Fourier transforms $g_j(k_i) = exp(-\sigma_i^2 k_i^2/2)$ of transverse (i=x,y) charge form factors (with $k_i \approx k\theta_i$), and of longitudinal form factor $F_z(k_z) = \exp(-\sigma_z^2 k_z^2/2)$, with $k_z \sim k$ since $\theta \ll 1$. If ***J(k)*** <<1 or $N_B \rightarrow 0$, only the incoherent OTR term ($\propto N$) remains in Eq. (2).

Now we will discuss the origin of Eq. (1) above for single particle OTR. The square of the perpendicularly polarized amplitudes for forward OTR from the first foil $\widehat{\boldsymbol{X}}_\perp$ and the backward OTR from the second foil $\widehat{\boldsymbol{A}}_\perp$ are given by [8]

$$\left|\widehat{\boldsymbol{X}}_\perp\right|^2 \approx \beta_\perp^2\left[\frac{4}{(\gamma^{-2}+\theta^2)^2} + \frac{4Re(r_\perp')}{(\gamma^{-2}+\theta^2)(1-\beta\,\theta)} + \frac{|r_\perp'|^2}{(1-\beta\,\theta)^2}\right]$$

$$\left|\widehat{\boldsymbol{A}}_\perp\right|^2 \approx \beta_\perp^2\left[\frac{4|r_\perp|^2}{(\gamma^{-2}+\theta^2)^2} + \frac{4Re(r_\perp)}{(\gamma^{-2}+\theta^2)(1-\beta\,\theta)} + \frac{1}{(1-\beta\,\theta)^2}\right]$$

where the reflectivity of the first and second foils are given by $|r_\perp'|^2$ and $|r_\perp|^2$, respectively and $\beta_\perp$ is the perpendicular component of the beam velocity $v_\perp/c$. The first terms in the equations above are of order γ^4 and the second term is of order γ^2, so we keep only the first term since $\gamma \gg 1$. Noting that the OTR from the first foil is reflected by the second foil we see that $|r_\perp|^2\left|\widehat{\boldsymbol{X}}_\perp\right|^2 = \left|\widehat{\boldsymbol{A}}_\perp\right|^2$, to highest order, so we obtain the result which is Eq. (1) above,

$$\frac{d^2W_{1\perp}(\theta)}{d\omega d\Omega} = \frac{e^2}{\hbar c}\frac{1}{4\pi^2\omega}\left|\widehat{\boldsymbol{A}}_\perp\right|^2 \approx \frac{e^2}{\hbar c}\frac{1}{\pi^2\omega}\,\beta_\perp^2\,\frac{|r_\perp|^2}{\left(\gamma^{-2}+\theta_x^2+\theta_y^2\right)^2}.$$

Thus, the amplitudes for OTR from the first and second foils in this approximation factor out of the interference expression ***I(k)*** in Eq. (3).

The formal convolution of Eq, (1) with the angular distributions of $\boldsymbol{\beta}$ modeled as normalized Gaussian distributions in x-angles α_x and y-angles α_y is expressed as

$$\left\langle\frac{d^2W_{1\perp}(\theta_x,\theta_y=0)}{d\omega d\Omega}\right\rangle = \frac{e^2}{\hbar c}\frac{1}{\pi^2\omega}\beta^2|r_\perp|^2\frac{1}{2\pi\sigma_x'\sigma_y'}$$
$$\times\iint d\alpha_x d\alpha_y\, e^{-\alpha_x{}^2/2\sigma_x'}\, e^{-\alpha_y{}^2/2\sigma_y'}\,\frac{\alpha_y^2}{\left[\gamma^{-2} + (\theta_x-\alpha_x)^2 + \alpha_y^2\right]^2}.$$

where we replaced $\beta_\perp^2$ by $\beta^2\alpha_y^2$ in Eq. (1). This convolution is now done numerically. Our previous approximate expression for the convolution over α_y valid for $\sigma_y' \ll 1/\gamma$ involved replacing the fraction in the integral above by

$$\frac{(\alpha_y)^2}{[\gamma^{-2} + (\theta_x-\alpha_x)^2]^2} \rightarrow \frac{(\sigma_y')^2}{[\gamma^{-2} + (\theta_x-\alpha_x)^2]^2},$$

where the r.h.s. above shows the result of the α_y integral.

APPLICATION OF NEW COTRI VERSION

Here we will compare the results of the numerical convolution for $I_\perp$ with the previous approximation valid for $\sigma_y' \ll 1/\gamma$. First we will show a beam parameter set relevant to LPAs [6].

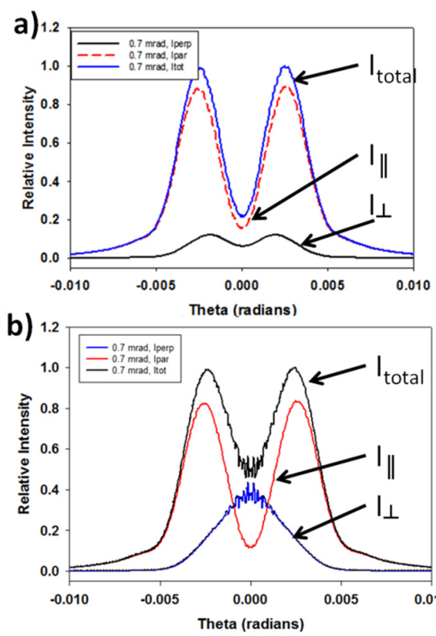

Figure 2: Comparison of a) numerical and b) approximate $I_\perp$ for a case relevant to LPA diagnostics with parameters E=1 GeV, $1/\gamma$=0.5 mrad, L=50.8 mm, λ=633 nm, beam divergence $\sigma'_{x,y}$=0.7 mrad, rms beam radii at foils #1 and #2 of 10 μm and 36.9 μm, total charge=235 pC, and bunching fraction=1% . Note $\sigma'_y > 1/\gamma$.

We see that the approximate treatment exaggerates the contribution of $I_\perp$ as compared to the numerical approach, which exhibits a two peaked $I_\perp$ for this divergence value. Also, there are strange oscillations at the peak of $I_\perp$ coming from the use of the approximate integrand for the α_x convolution. Note that $I_\parallel$ is unchanged in Figs. 2a) and b) as one would expect. In practice the numerical convolutions in α_x and α_y are applied to the entire COTRI model, Eq. (2).

ISBN: 978-3-95450-214-1 ISSN: 2673-5490 doi:10.18429/JACoW-IPAC2021-TUPAB275

Next, in Fig. 3, we show $I_{total} = I_{\parallel} + I_{\perp}$ for the same beam parameters as in Fig. 2, except that the beam divergences range from 0.1 to 0.7 mrad, as compared to 1/γ=0.5 mrad. The valley around θ=0 is considerably more filled-in for the case of the approximate $I_{\perp}$ in Fig. 3b), especially for the larger divergences. The lowest two divergences are similar in Figs. 3a) and b).

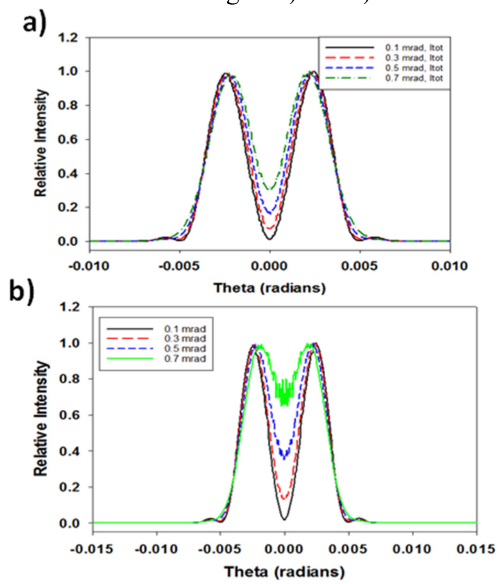

Figure 3: Plots of $I_{total} = I_{\parallel} + I_{\perp}$ using a) the new numerical $I_{\perp}$ and b) the approximate $I_{\perp}$, having beam parameters as in the previous slide, except divergence σ'_y=0.1, 0.3, 0.5, and 0.7 mrad, and the beam radius at foil #1 is 30 μm. The beam radius at foil #2 varies with divergence. Note the different θ-scale in b).

Figure 4 illustrates the application of COTRI to cases of potential interest for pre-bunched FELs, where microbunching diagnostics of modulator output with very high bunching fractions could be employed, consequently yielding large gains in the coherent OTR. Figure 4a) shows I_{total} for two beam sizes, σx,,y =10 μm and 100 μm. The divergence $\sigma'_{x,y}$=0.1 mrad was the same in both cases. The smaller beam radius produces coherent OTR radiation out to relatively larger angles because the coherence factor is large there and several interference fringes are seen. In the larger beam radius case coherent radiation is suppressed, except at very small angles near θ=0. Note that the two examples in Fig. 4a) are normalized to unity here so the actual coherent intensities in these two plots can't be compared directly. For example the relative level of COTR in the valley of the 100 μm is distorted by the normalization as compared to the 10 μm case. The COTR gains for these parameters were ~106. Figure 4b) shows a set of COTRI plots, all for a beam size of σx,y =10 μm. The effect of divergence on the far field interference pattern is clearly demonstrated there.

CONCLUSIONS

Optical transition radiation based diagnostic techniques provide valuable information on beam properties. Near field imaging gives beam size even to the order of microns, while the far field COTRI technique measures the beam divergence in both x- and y- angles using polarized OTR. Thus, beam emittances can be determined when at a beam waist. The far field gives information on the angular trajectory of the beam. Both near- and far-field imaging give information about the bunching fraction of

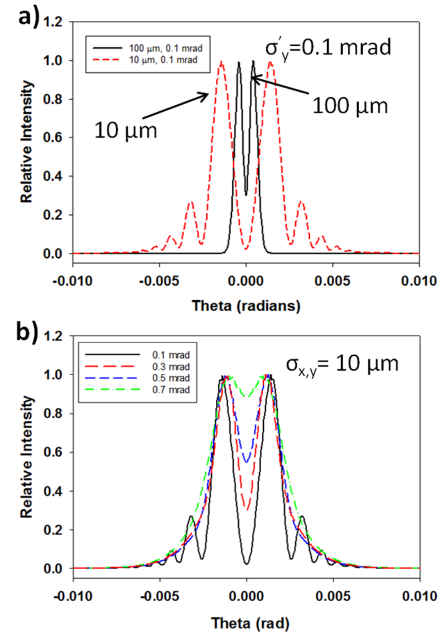

Figure 4: Plots of $I_{total} = I_{\parallel} + I_{\perp}$ for a) two beams with sizes σx,y=10 μm and 100 μm, both with divergence σ'x,y= 0.1 mrad, and b) beams all with size σx,y=10 μm and divergences σ'x,y= 0,1, 0,3, 0,5 and 0.7 mrad. The common parameters used in a) and b) are E=375 MeV, 1/γ=1.36 mrad, L=63 mm, λ=266 nm, total charge=300 pC, and bunching fraction=10%.

microbunched beams from the coherent OTR gain. These techniques have been successfully used for FEL and laser plasma accelerator beam diagnostics. The examples shown here indicate that COTRI would be of interest for pre-bunched FEL diagnostics also. The new numerical treatment for the perpendicular polarization of OTR enlarges the range of beam divergences that can be accurately modeled to $\sigma'_{x,y} > \gamma^{-1}$.

ACKNOWLEDGEMENTS

The co-author acknowledges the support of J. Byrd and M. Borland of the Accelerator Systems Division at ANL. D. W. R. gratefully acknowledges the sustained support and encouragement by Carleen Rule.

The submitted manuscript has been created by UChicago Argonne, LLC, Operator of Argonne National Laboratory (Argonne). Argonne, a U.S. Department of Energy Office of Science Laboratory, is operated under Contract No. DE-AC02-06CH11357. The U.S. Government retains for itself, and others acting on its behalf, a paid-up nonexclusive, irrevocable worldwide license in said article to reproduce, prepare derivative works, distribute copies to the public, and perform publicly and display publicly, by or on behalf of the Government.

ISBN: 978-3-95450-214-1 ISSN: 2673-5490 doi:10.18429/JACoW-IPAC2021-TUPAB275

REFERENCES

[1] D.W. Rule and A.H. Lumpkin, "Analysis of Coherent Optical Transition Radiation Interference Patterns Produced by SASE-Induced Microbunches," in *Proc. 19th Particle Accelerator Conf. (PAC'01)*, Chicago, IL, USA, Jun. 2001, paper TPAH029, pp 1288-1290.

[2] A. H. Lumpkin *et al.*, "Evidence for Microbunching Sidebands in a Saturated Free-electron Laser Using Coherent Optical Transition Radiation," *Phys. Rev. Lett.* vol. 88, no. 23, p. 234801, May 2002. doi:10.1103/PhysRevLett.88.234801

[3] Y. Glinec *et al.*, "Observation of Fine structures in Laser-driven Electron beams Using Coherent Transition Radiation," *Phys. Rev. Lett.* vol. 98, no. 19, p. 194801, May 2007. doi:10.1103/PhysRevLett.98.194801

[4] C. Lin *et al*., "Long-Range Persistence of Femtosecond Modulations on Laser-Plasma-Accelerated Electron Beams," *Phys. Rev. Lett.* vol. 108, no 9, p. 094801, Mar. 2012. doi:10.1103/PhysRevLett.108.094801

[5] A.H. Lumpkin *et al.*, "Observations of Coherent Optical Transition Radiation Interference Fringes Generated by Laser Plasma Accelerator Electron Beamlets," in *Proc. AAC18,* Breckenridge CO, USA, Aug. 2018. doi:10.1109/AAC.2018.8659381

[6] A. H. Lumpkin *et al.*, "Coherent Optical Signatures of Electron Microbunching in Laser-Driven Plasma Accelerators," *Phys. Rev. Lett.,* vol. 125, no. 1, p. 014801, Jul. 2020. doi:10.1103/PhysRevLett.125.014801

[7] L. Wartski *et al.*, "Interference phenomenon in optical transition radiation and its application to particle beam diagnostics and multiple-scattering measurements", *J. Appl. Phys.* vol. 46, no. 8, p. 3644, Aug.1975. doi.org/10.1063/1.322092

[8] L. Wartski, "Study of the Optical Transition Radiation Produced by 30 to 70 MeV Electrons, Application to Diag-nostics of Beams of Charged Particles," thesis, D. Phys. Sc., Université de Paris-Sud, Centre d'Orsay, Paris, France, 1976.